Senior Thesis

Pressure-Temperature Conditions of Granulite Formation in Rogaland, SW Norway

by

Katrina Edwards

1994

Submitted as partial fulfillment
of the requirements for the degree
of Bachelor of Sciences at
The Ohio State University
Spring Quarter, 1994

Approved By:

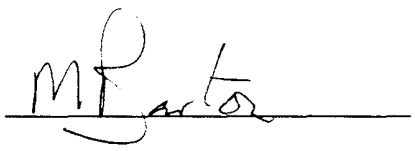

Dr. Michael Barton

TABLE OF CONTENTS

ABSTRACT

The geology of SW Norway is dominated by high-grade amphibolite to granulite facies gneisses with associated migmatites and anorthosite-magerite complexes. Previous work suggests that metamorphism consisted of two high temperature events at 1.45 Ga (M1) and 1.0 Ga (M2), followed by regional cooling and formation of retrograde assemblages (M3). Partial reequilibration of certain mineral phases has led to some uncertainty about the pressures of metamorphism and whether the retrograde assemblages represent a discrete metamorphic event. Pressure and temperature conditions of the M2 metamorphism of gneisses located near the osumilite-in isograd were constrained using gt-opx, opx-bt, cord-bt-gt, and gt-sill-qt-plag equilibria. Core compositions were used for all ferromagnesium phases to avoid the effects of Fe-Mg exchange during cooling. Results suggest that peak metamorphism occurred at pressures of 5-6 kb and temperatures of 710-800°C. Rim temperatures and pressures were estimated at 490-550°C and 4-5 kb, suggesting retrograde metamorphism, and possibly implying isobaric cooling.

INTRODUCTION

A primary concern for a metamorphic petrologist is understanding the formation and evolution of the continental crust. The middle to lower continental crust is composed largely of granulites. Granulites are a suite of high-grade metamorphic rocks that form at temperatures ranging from 700 to 1000 C°, and pressures from 4-12 kb, depending on the terrane (Bohlen, 1991). Studies of granulite terranes are therefore essential to understand the origin and evolution of the crust. Research over the past ten years suggests that granulites can form through tectonic processes, such as crustal thickening, or through the addition of heat via magma or fluid advection (Bohlen, 1991, Newton, 1990, Thompson, 1990). However, many details of the formation of granulites are poorly understood. Some unresolved questions include: Are granulites which are exposed at the surface chemically identical to lower crustal granulites? Have granulite terranes been exposed to pervasive fluid flow? To what extent has the mineralogy and geochemistry of exposed granulites been altered during retrograde metamorphism? An important key to granulite petrogenesis is determining the temperature and pressure conditions of granulite formation. Thermobarometry involves calculation of pressure and temperature (P-T) conditions reflected in the composition of minerals formed during metamorphism. Ideally, the minerals preserve equilibrium compositions. Usually this P-T condition is near the thermal peak because prograde metamorphic reactions equilibrate more rapidly than retrograde reactions.

This paper focuses on a quantitative petrological study of granulite metamorphism,

involving the determination of P-T conditions of metamorphism, for granulite samples collected from the Rogaland/Vest Ager region of SW Norway. This is a classic example of an amphibolite/granulite facies transition, and is well suited for study because of good exposure and accessibility, and because the general field relations have been well studied. P-T conditions are not well established for these granulites. A complicated metamorphic history and pervasive retrograde metamorphism have made it difficult to obtain samples that preserve the "peak" metamorphic conditions. Samples with mineral assemblages suitable for thermobarometry were collected from the Gydal Valley (35 km NW of Egersund). For this study, three thin sections have been selected for quantitative microprobe analysis, based on mineral assemblages expected to produce well-constrained pressures and temperatures. Thermobarometric calculations are made for this study using TWEEQU, a computer program written by Robert G. Berman, which uses an internally-consistent set of standard state thermodynamic data (Berman, 1991).

THE ROGALAND/VEST AGDER GRANULITE TERRANE: GENERAL GEOLOGY

Several major crust forming events between 3.5 and 1.5 Ga caused concentric growth of the Baltic Shield form an Archean crustal nucleus (Gaal and Gorbatshev, 1987). In SW Norway this was followed by the Sveconorwegian orogeny (1.25-0.87 Ga) related to the rifting of Laurentia from the Baltic shield, then re-closure of the ocean basin (Gaal and

Gorbatschev, 1987). Reworking of the older basement during this event involved high-grade (upper amphibolite-granulite facies) metamorphism, and was accompanied by intrusion of large volumes of magma. The geologic evolution between 1.25 and 0.4 Ga is discussed in Barton et al. (1991) from which the following summary is taken.

The high-grade metamorphic complex (Figure 1) consists of charnockitic and granitic gneisses, garnetiferous gneisses and augen gneisses intruded by magmas ranging in composition from anorthosite to granite. Metamorphic grade increases toward the igneous complex. The amphibolite facies occurs in the east, and increases to granulite facies in the west (Figure 1). Igneous and metamorphic activity spanned over one billion years of Earth history, from 1.5 Ga to 0.44 Ga (Demaiffe and Michot, 1985).

Previous work in Norway has sought to characterize the pressure, temperature, fluid compositions, and timing of metamorphic events. Kars et al. (1980), Jansen et al. (1985) and Tobi et al. (1985) have described four discrete metamorphic events (Fig.2). Two of the described events (M1 and M2) reflect high-grade (upper amphibolite to granulite facies) metamorphism associated with intrusion of anorthositic-leuconoritic-noritic-monzonortic magmas. Jansen et al. (1985) estimate pressures of 3-4 kb and temperatures of 750-1050°C for M2, with higher temperatures recorded by assemblages close to the intrusive complex (Figure 2a). Wilmart and Duchesne (1987) suggest pressures of 6-7.5 kb for crystallization of the upper part of the Bjerkeim-Sokndal lopolith (Figure 2b). More recent work by Miller et al. (1992) constrain pressure and temperature of the M2 event near the amphibolite-granulite facies transition using opx-bt, cpx-plag, amph-plag, and two-pyroxene equilibria. Their results indicate that metamorphism occurred at pressures of 3.5-5 kb and temperatures of 780-

820°C. Calculated pressures and temperatures range between 3-7.5 kb, and 750-1050°C, depending on proximity to the intrusive complex. The M3 event records regional cooling following the peak M2 conditions during slow regional uplift (Maijer et al., 1981; Huijsmans et al. 1982). Mineral assemblages have been extensively re-equilibrated at pressures of 3.5-5 kb and temperatures of 650-750°C (Miller et al., 1992). The M4 event is related to the Caledonian orogeny following opening then closure of Iapetus and produced localized prehnite-pumpellyite to lower greenshist facies assemblages (Sauter et al. 1983; Barton and Van Bergen, 1984).

P-T-t data for Rogaland/Vest Agder are consistent with a clockwise path (Figure 3), which typically results from continental collision and crustal thickening. An inferred Proterozoic crustal thickness of 50-60 km (Demaiffe and Michot, 1985), together with recumbent folding during early high-grade metamorphism (Michot, 1969; Hermans et al., 1975; Huijsmans et al., 1981) is consistent with crustal thickening resulting from subduction with plate collision (Falkum and Petersen, 1980; Falkum, 1987), obduction with plate collision (Demaiffe and Michot, 1985), or lithospheric doubling (Vlaar, 1985). The exact P-T trajectory of the retrograde path is uncertain, but cooling was nearly isobaric (Jansen et al., 1985). This suggests that extension followed thickening, and was probably important for the emplacement of the Hunnedalen dike system about 900 Ma (Barton et al., 1991).

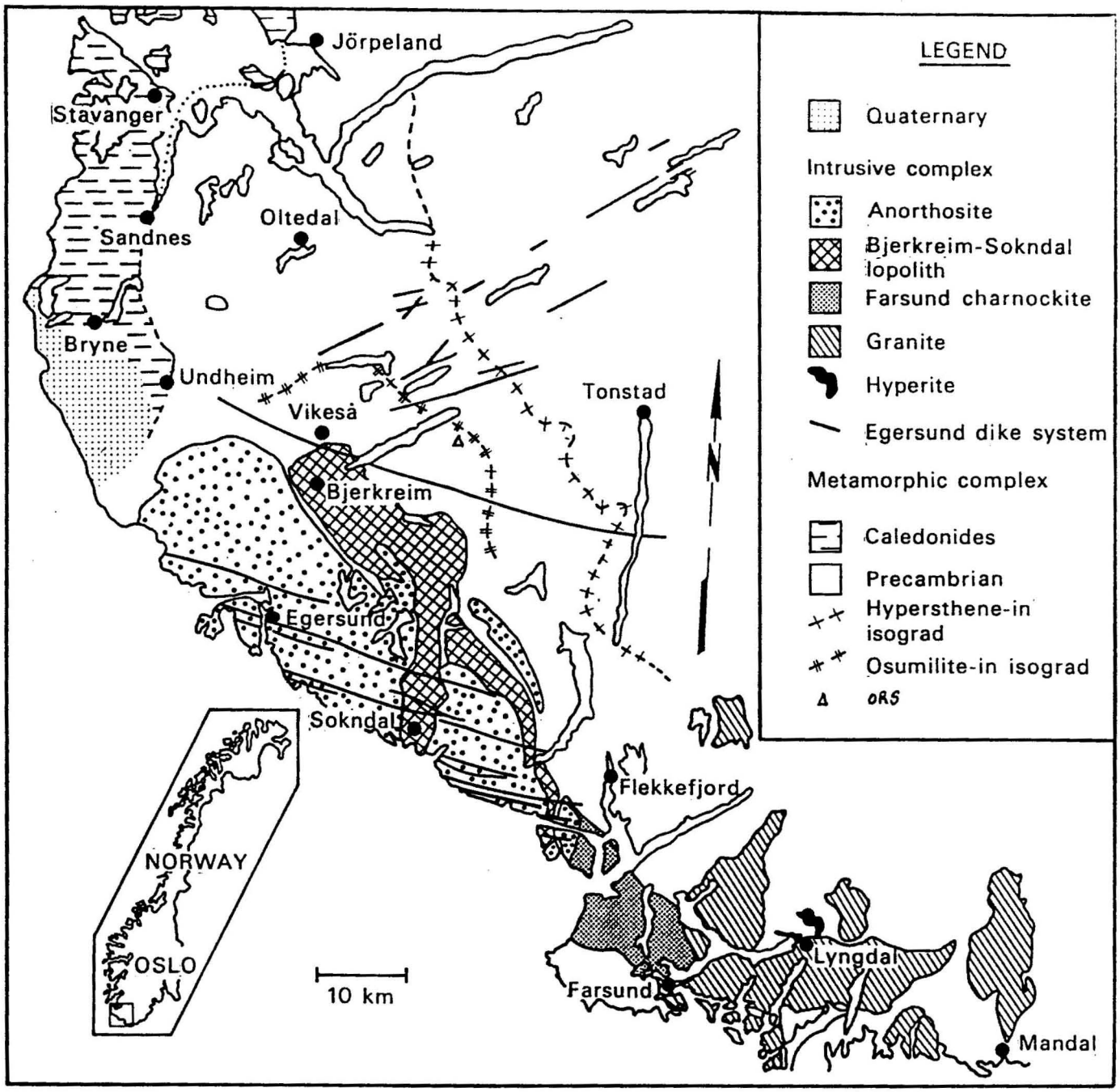

Figure 1: Geologic map of Rogaland/Vest Agder showing the distribution of the major intrusive bodies (from Barton and Van Gaans, 1988). The hyperstherne-in isograd for leucocratic rocks is from Hermans et al. (1975) whereas the osumilite-in isograd is from Maijer et al. (1981). The Hunnedalen dikes trend NE-SW. Locale of rocks collected for this study are labled ORS.

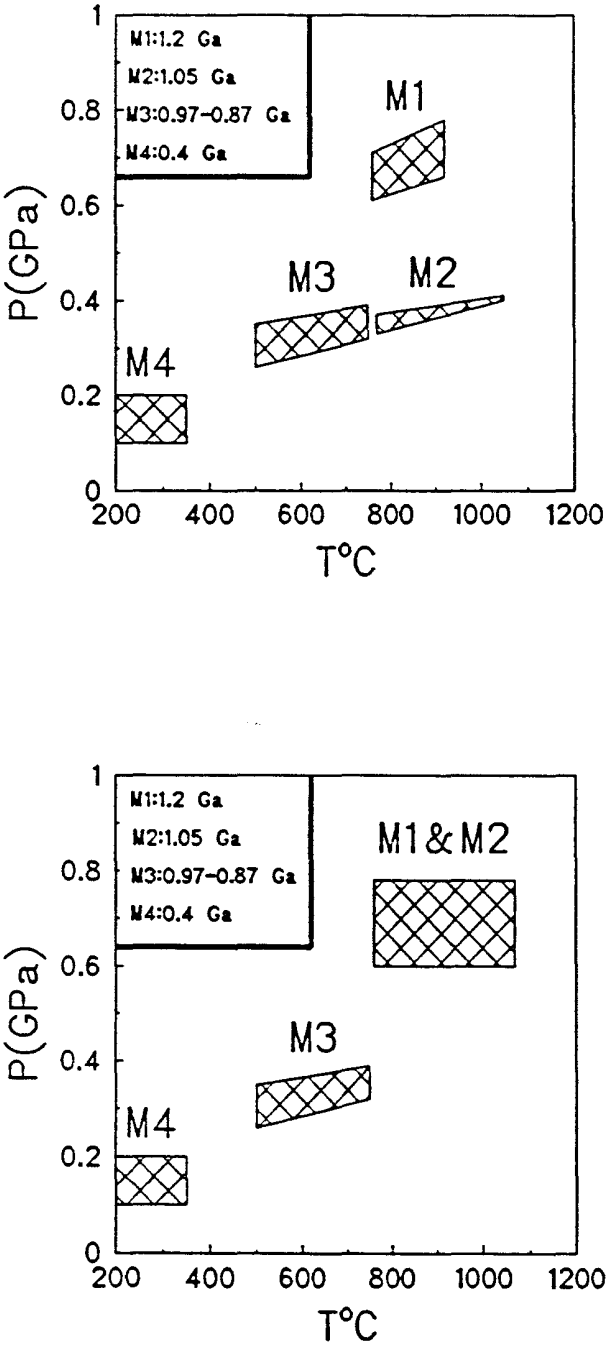

Figure 2: Summary of ages and P-T estimates of metamorphism for Rogaland/Vest Ager compiled from sources listed in the text. **Upper diagram** shows P-T estimates of Jansen et al. (1985) for the M2 event, whereas the **lower diagram** shows the pressure estimate of Wilmart and Duchesne (1987) for this event.

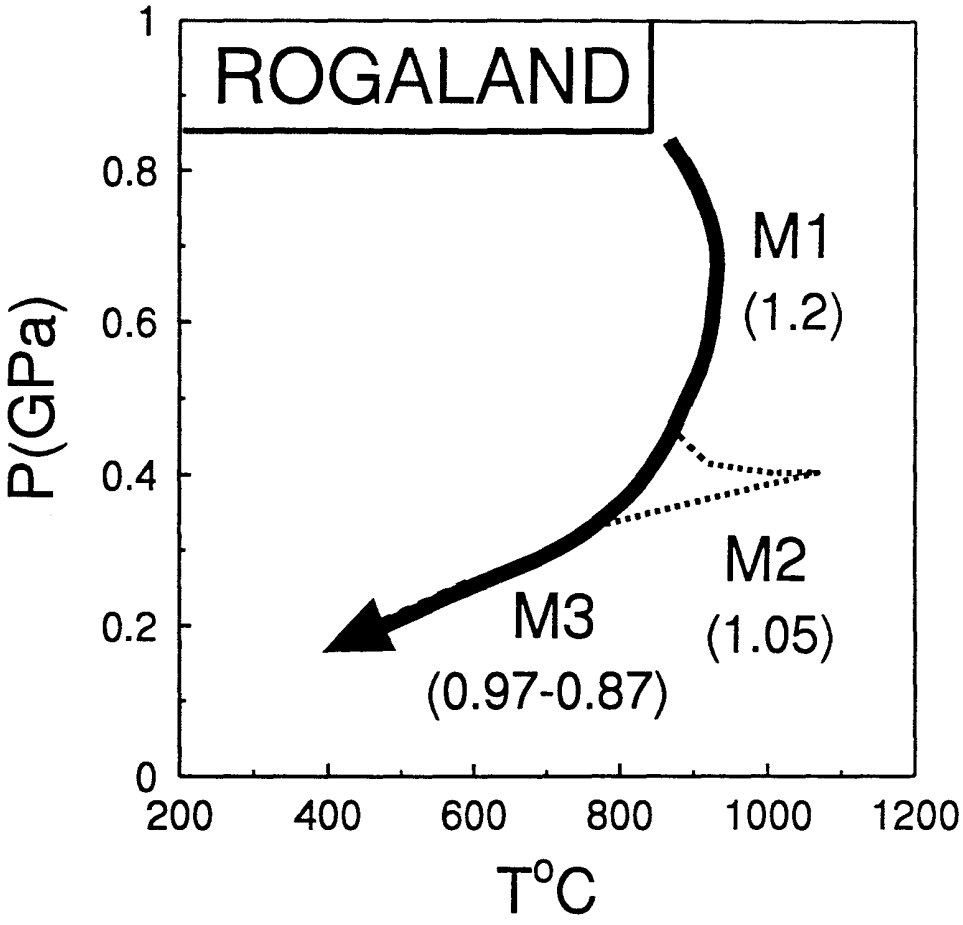

Figure 3: Generalized P-T-t path based on quantitative estimates from Miller et al. (1992).

ANALYTICAL PROCEDURES

Minerals in selected samples were analyzed with a Cameca SX-50 microprobe. Representative analyses are in Appendix A. Compositions were determined using a one micron spot, an excitation voltage of 15 kV, and beam current of 20 nA for all minerals except feldspar. Feldspar was analyzed using a de-focused beam of five microns, and a current of 15 nA, to avoid beam-induced Na migration. Count times varied between 10 and 40 seconds, depending on the concentration of the element being analyzed. Elements in low concentrations were analyzed for longer count times than elements in high concentration. ZAF corrections were made using software provided by Cameca.

Minerals for analysis were selected and mapped using thin section enlargements made using a microfiche photocopier. Minerals were primarily selected for their lack of apparent alteration, and textural equilibrium. To avoid the effects of Fe-Mg exchange between the ferromagnesium phases, only the cores of isolated grains were selected for computational purposes. Rims of these grains were analyzed for comparative purposes. Complete thin-section descriptions can be found in Appendix B.

Garnet zoning was assessed by analyzing spots on a traverse through several crystals, of variable sizes, from each section. Line traverses were made along two perpendicular traverses from the center to the edge of the crystal. Spots were analyzed approximately every 100 microns, unless an inclusion occured along the traverse. For samples with significantly different rim and core compositions (garnet, biotite, orthopyroxene), both compositions are

reported. Core and rim compositions were also determined in cordierite, but showed no variation. Core and rim compositions were determined by averaging counts on at least three spots of the core or rim of the mineral. Pressure and temperature calculations were made using Robert Berman's program, TWEEQU (Thermobarometry With Estimation of EQUilibtation state; Berman, 1991). TWEEQU calculations are made by using a set of internally consistent thermodynamic data for end members and solution properties, so that thermobarometric consistency is guaranteed (Berman, 1991). The thermobarometric method used here presents all solutions, both graphically, as in P-T activity diagrams, and analytically, based on the graphical results. Details of the various algorithms used by this software can be found in Brown et al. (1988). If it is assumed that thermodynamic and compositional data are without errors, a set of minerals in equilibrium with each other will intersect at a single point in P-T space. Under these conditions, TWEEQU can calculate peak metamorphic temperatures and pressures. However, a set of mineral **not** in equilibrium will display multiple intersections at different pressures and temperatures. The degree to which multiple intersections converge at to single point in P-T space can be indicative of the degree to which the system is in equilibrium. Thus, TWEEQU is also a powerful tool for identifying and evaluating mineral disequilibrium in a system.

DATA ANALYSIS

Compositional zoning of garnets, biotites, and orthopyroxenes has been examined (see

appendix A). Garnets are almandine-rich (Alm_{66}-Alm_{73}), have pyrope contents ranging from Pyr_{23} to Pyr_{29}, and usually have less than 7 percent total spessartine + grossular. Most garnets in the thin studied sections are >2 mm diameter, and showed a moderate degree of zoning, which becomes more apparent as the size of the garnet increases. The garnets all displayed similar zoning characteristics, where Mg is concentrated in the cores compared with the rims, while Fe shows an opposite sense of enrichment. Ca and Mn do not display consistent patterns of zoning. Line transects found the garnets to be essentially homogeneous over a broad region of the core, while compositions change rapidly near the rim. Figure 4 shows zoning profiles for a typical garnet in sample 1.

Biotites and orthopyroxenes were chosen for analysis that were not in contact with any other iron-bearing phases. Both biotite and orthopyroxene grains are around 1-2 mm diameter, are compositionally zoned, but homogeneous throughout the samples. Biotite cores are Mg-poor and Fe-rich compared with the rims. Orthopyroxene cores are Ca-Mg-poor and Fe-rich, compared with the rims.

All combinations of cores and rims, as well as average compositions were plotted using TWEEQU to find the maximum and minimum temperatures and pressures, and combinations of phases that could represent assembleges in equilibrium. Maximum temperatures occur in the range 710-800°C, while maximum pressures occur between 5.1-5.5 kb. The maximums were obtained using core compositions for all phases. Minimum temperatures of about 490-550°C, and minimum pressures of 4.5-4.8 kb were found using rim compositions for all phases. These temperatures and pressure were consistent throughout all of the sections. A summary of results for each section follows:

Sample 1: Figures 5a and 5b display the P-T plots for the respective core and rim analyses. Corresponding computations of average pressures and temperatures derived from this and other P-T plots are as follows. The mineral assemblage used for the calculations in this section included biotite, cordierite, garnet, sillimanite, and quartz. Core and rim temperatures and pressures for this sample are respectively 710°C, 5.3kb, 510°C, 4.5 kb.

Sample 2: Figures 6a and 6b show the P-T plots for this sample. The mineral assemblage used for calculations in this sample consisted of biotite, garnet, and orthopyroxene. The thermometers used in this section are close only when core compositions are used. Rim compositions yields widely divergent temperature plots. Overlaying barometers used in samples 1 and 3 (figure 6c) give a temperature range of 690-730°C, and a pressure range of 4.9-5.3 for core compositions in this sample.

Sample 3: P-T calculations for sample 3 were made with the mineral assemblage biotite-corderite-garnet-plagioclase-sillimanite-quartz. Figures 7a and 7b show plots of core and rim compositions, as before. The intersections corresponding to biotite-corderite-garnet-sillimanite-quartz occur at very similar pressures and temperatures as sample 1. However, several other intersections appear in this graph, most of them involving plagioclase. Main intersections occur at temperatures and pressures of 760°C, 5.2 kb, 720°C, 9.1 kb, 950°C, 5.4 kb, and 1050°C, 3.7 kb (cores only). The first temperature and pressure correspond to the bt-cord-gt-sill-qt intersection. Multiple equilibria suggest that at least one phase is out of equilibrium with the others.

Figures 5, 6, and 7 were made with the assumption that the ratio of Fe^{3+}/Fe^{2+} concentrations in garnets was zero. Temperatures obtained when the iron is assumed to be

ferrous are higher (McGuire et al., 1989), and thought to be more reliable (Griffin et al., 1984). Methods for calculating ferric iron content have also been disputed by McGuire et al. (1989), as it has been shown by Mössbauer spectroscopy that measured Fe^{3+} contents do not agree with the Fe^{3+} contents calculated from the stoichiometry of microprobe analyses. A sample plot was made to show the effect ferric iron has on these thermobarometric calculations. Figure 8 plots the same mineral compositions as figure 7a, excepting garnet, which has been recalculated to account for ferric iron. The Fe^{+3} contents were determined based on stoichiometry (Fe^{+3}=2-Al+Ti+Cr). The results obtained are comparable to figure 7a, temperature varying only about 25°C (lower), and pressure increasing less than 0.5 kb with the ferric iron correction. This indicates that the garnet analyzed in this study is near stoichiometric and does not contain a signifigant amount of ferric iron.

RESULTS AND DISCUSSION

It is clear from examining figures 5a, and 7a, that biotite, cordierite, and garnet are in equilibrium in these samples, as implied by consistent intersections obtained on several thin sections. The concurrent temperatures and pressures obtained using this system lends validity to the analytical procedures, mineral compositions used, and to the temperatures and pressures they reflect. Additionally, results from sample 2 appear to be in equilibrium, and reflect similar temperatures as those from samples 1 and 3 when their barometers are overlaid.

Figure 7a displays multiple discordant intersections, reflecting a system out of

equilibrium. The curve for the GASP barometer (garnet-aluminosilicate-silica-plagioclase) plots far from the intersection defined by curves for other equilibria. Garnet, by comparison with other graphs (see figures 5a and 6a), appears to be in equilibrium with biotite and cordierite. Thus by default it was concluded that plagioclase was most likely the culprit for the state of disequilibrium displayed in figures 7a and 7b. Plagioclase compositions for this sample are generally around Ab_{60}-Ab_{65}, An_{34}-An_{40}. By manipulating the anorthite and albite components, figures 7c and 7d were obtained. Increasing the anorthite component (An_{45}, Ab_{55}) resulted in a greater spread in temperatures and pressures for all intersections except the central intersection. The central intersection represents the gt-bt-sill-cord equilibria, which does not contain plagioclase and is therefore unaffected (see figure 7c). Decreasing the anorthite component (An_{25}, Ab_{74}) brought all of the intersections to roughly the same position as the one involving gt-bt-sill-cord ($\mp$25°C, 0.5 kb). Figure 7d shows this relationship.

There are several possible explanations for this result. One is that Na migrated out of the feldspar during retrograde metamorphism, or during analysis. However, this seems unlikely because Al would have had to diffuse into the grains in order to maintain stoichiometry. Al is not considered a very mobile element under these conditions, and because the stoichiometry of the plagioclase was near-perfect, there is no evidence to support a diffusion hypothesis. Another possible explanation is based on textural evidence. All plagioclase crystals in this sample are small (approximately 1 mm diameter), and usually were found in a region of highly altered cordierite. It is suggested, then, that the plagioclase crystals were formerly inclusions in preexisting cordierite, and were thus inhibited from reaching equilibrium with the rest of the system. Whatever the actual reason for this apparent disequilibrium, the

intersections do not represent a realistic option for temperatures and pressures of the M2 metamorphic event. At temperatures and pressures of about 900-1000°C, 5-9kb, melting would have been occurring even under anhydrous conditions, for which no evidence is found at this locale.

Figure 4: Garnet zoning profile, sample 1

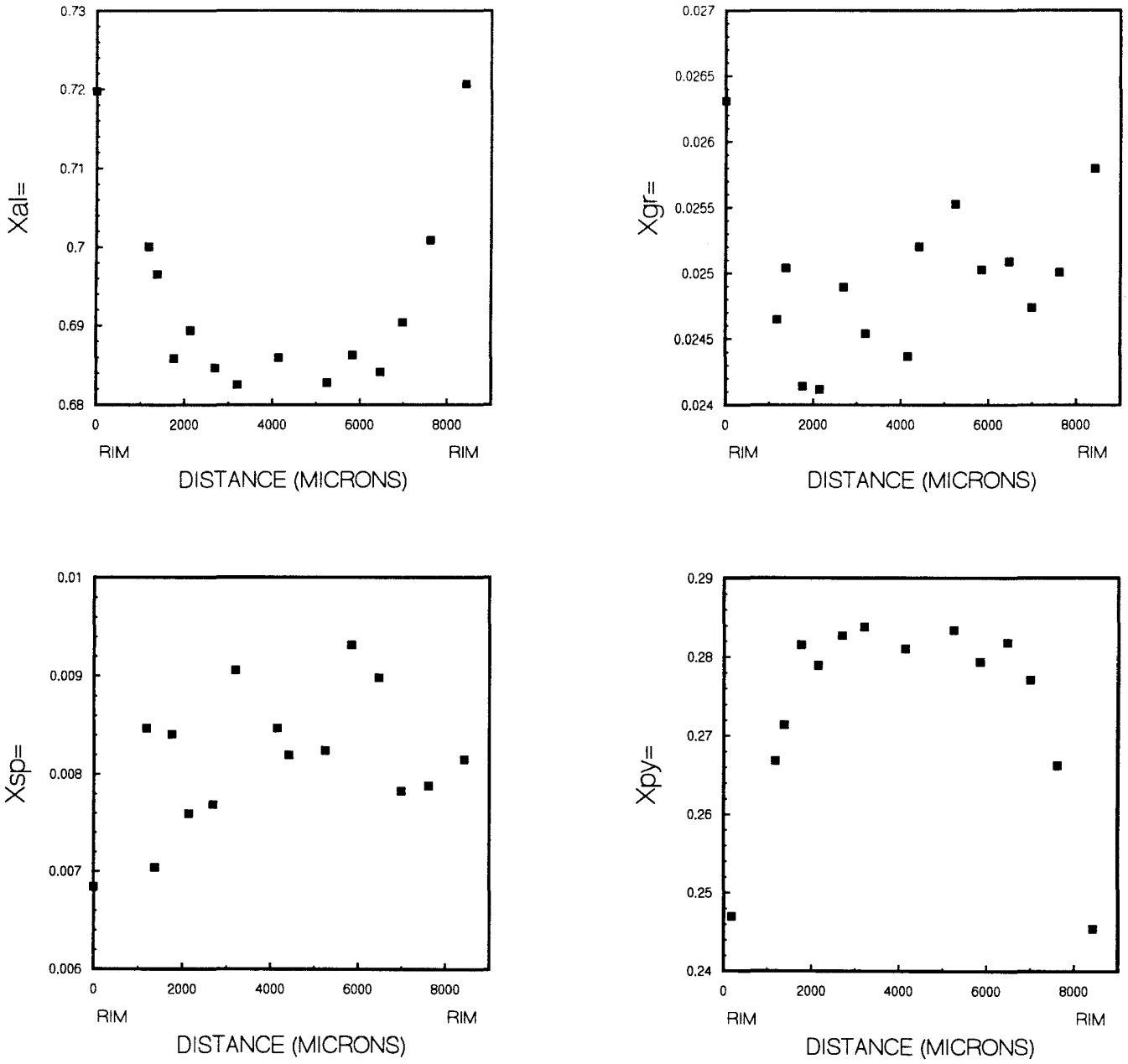

Figure 5a: TWEEQU plot from sample 1, representing core compositions

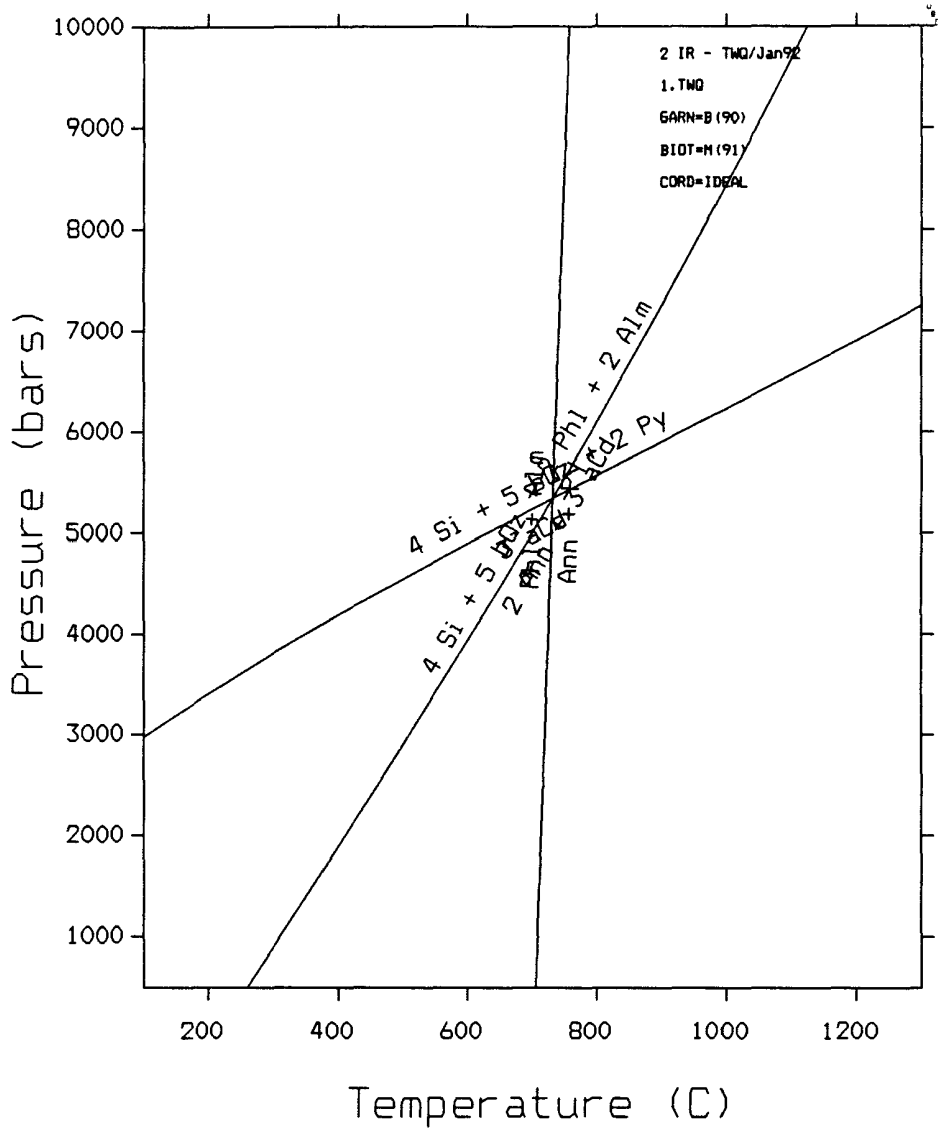

Figure 5b: TWEEQU plot from sample 1, representing rim compositions

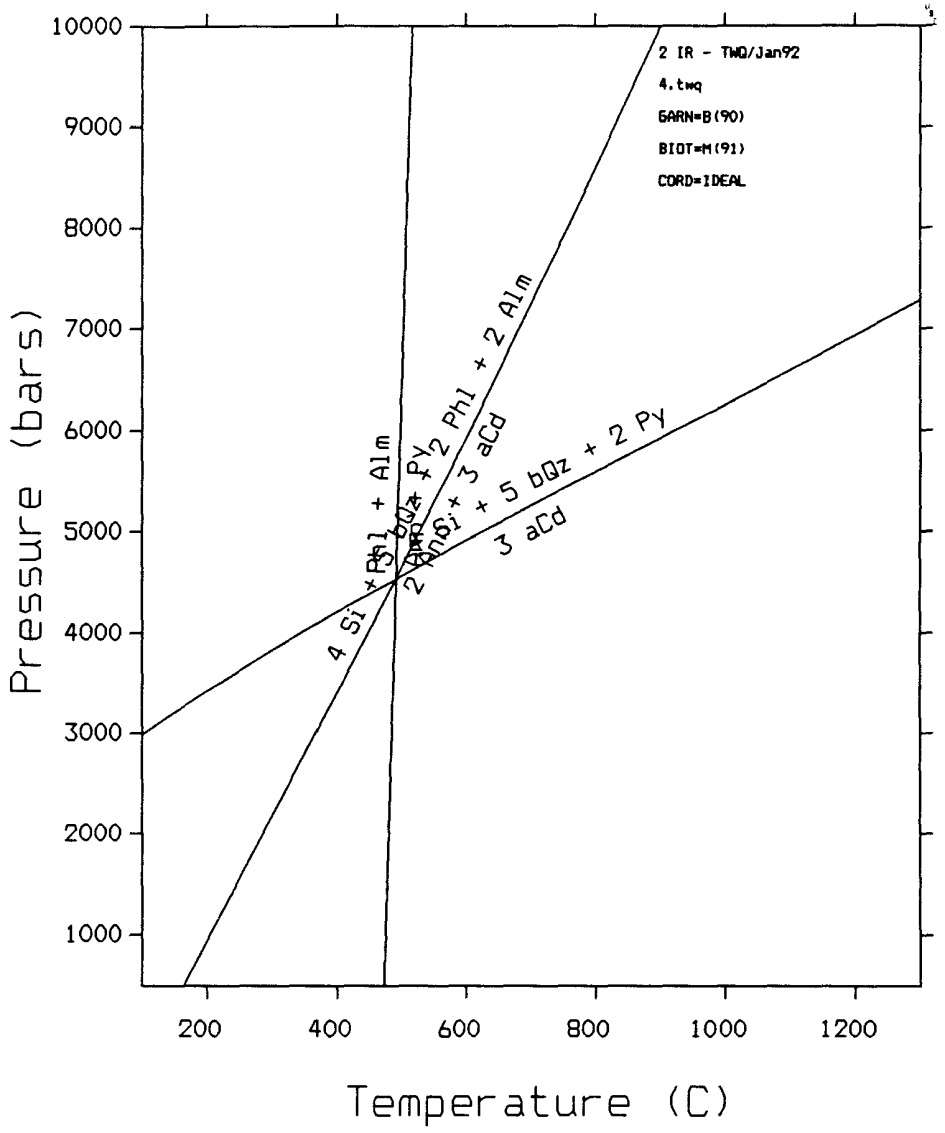

Figure 6a: TWEEQU plot from sample 2, representing core compositions

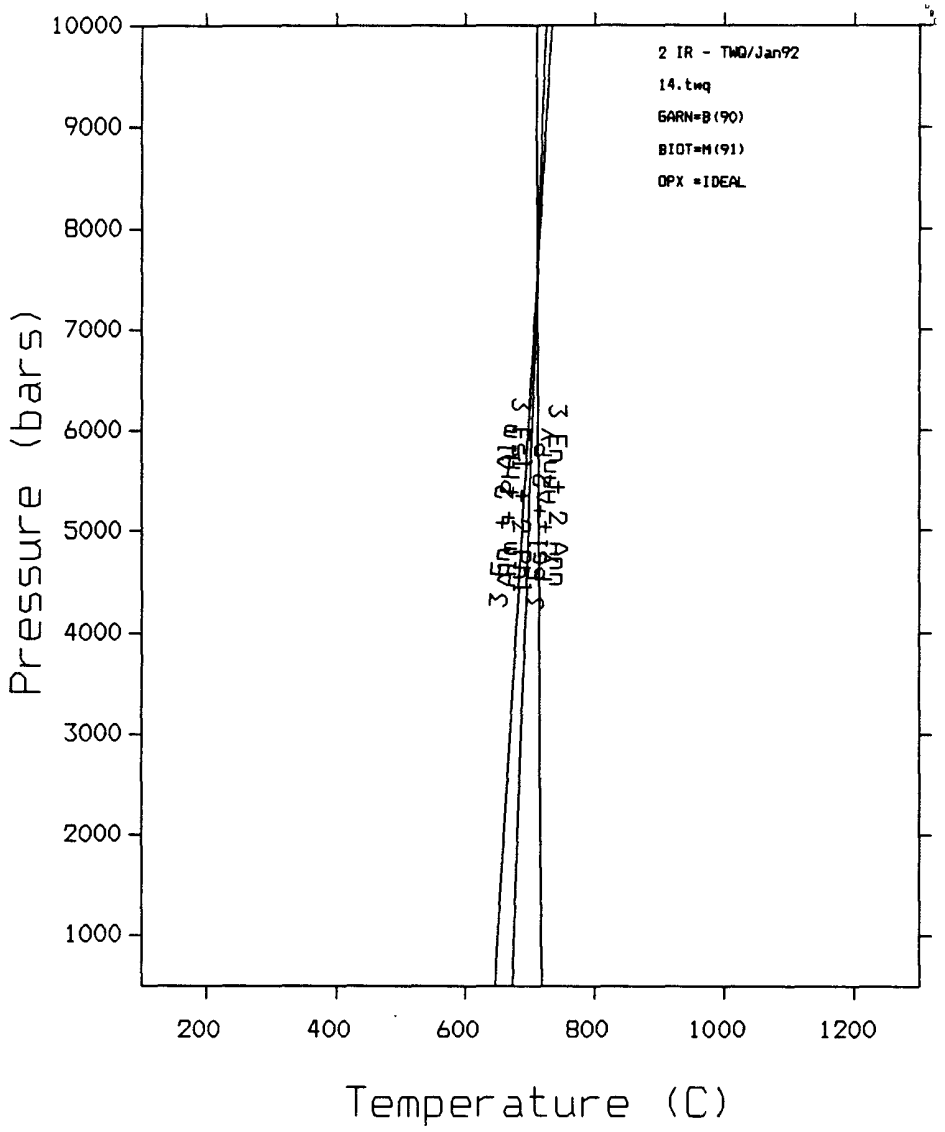

Figure 6b: TWEEQU plot from sample 2, representing rim compositions

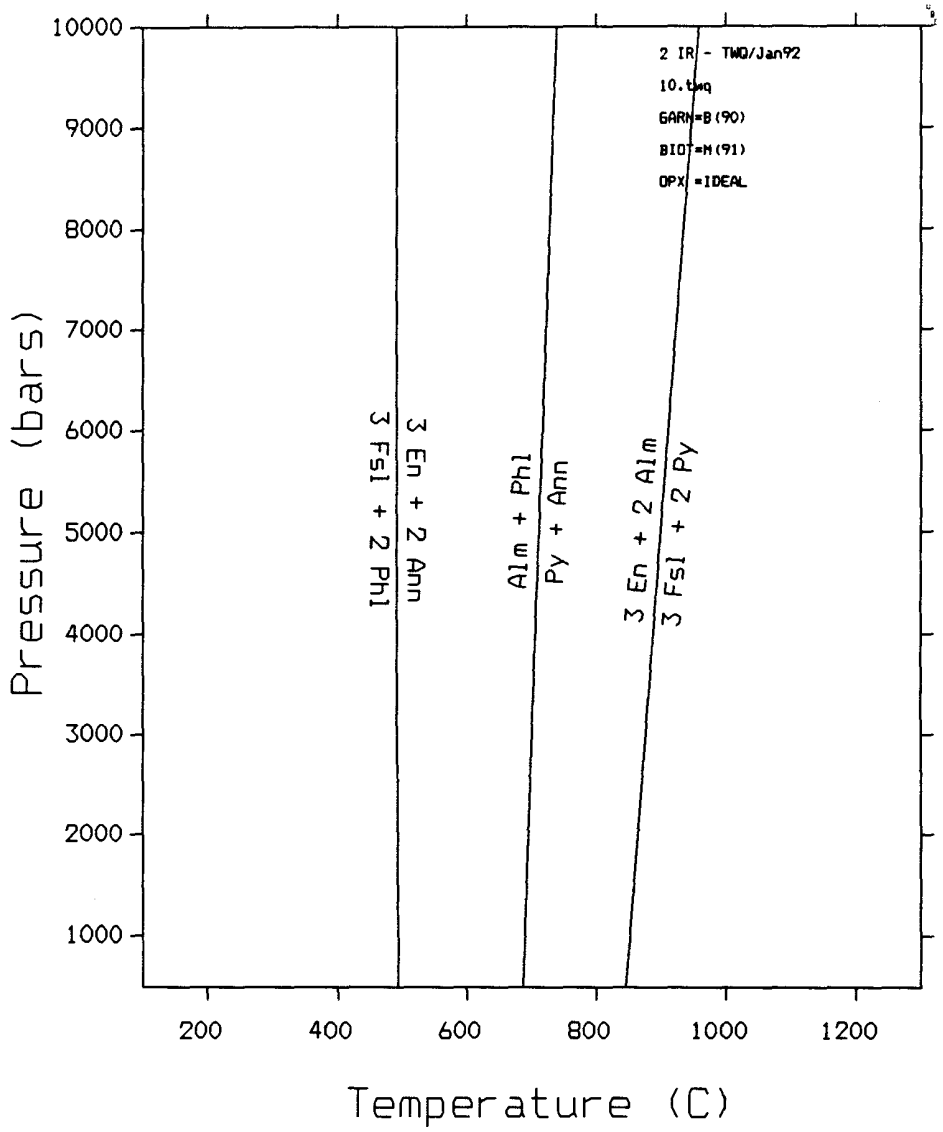

Figure 6c: TWEEQU plot representing core compositions of sample 2, overlaid by core compositions of sample 1

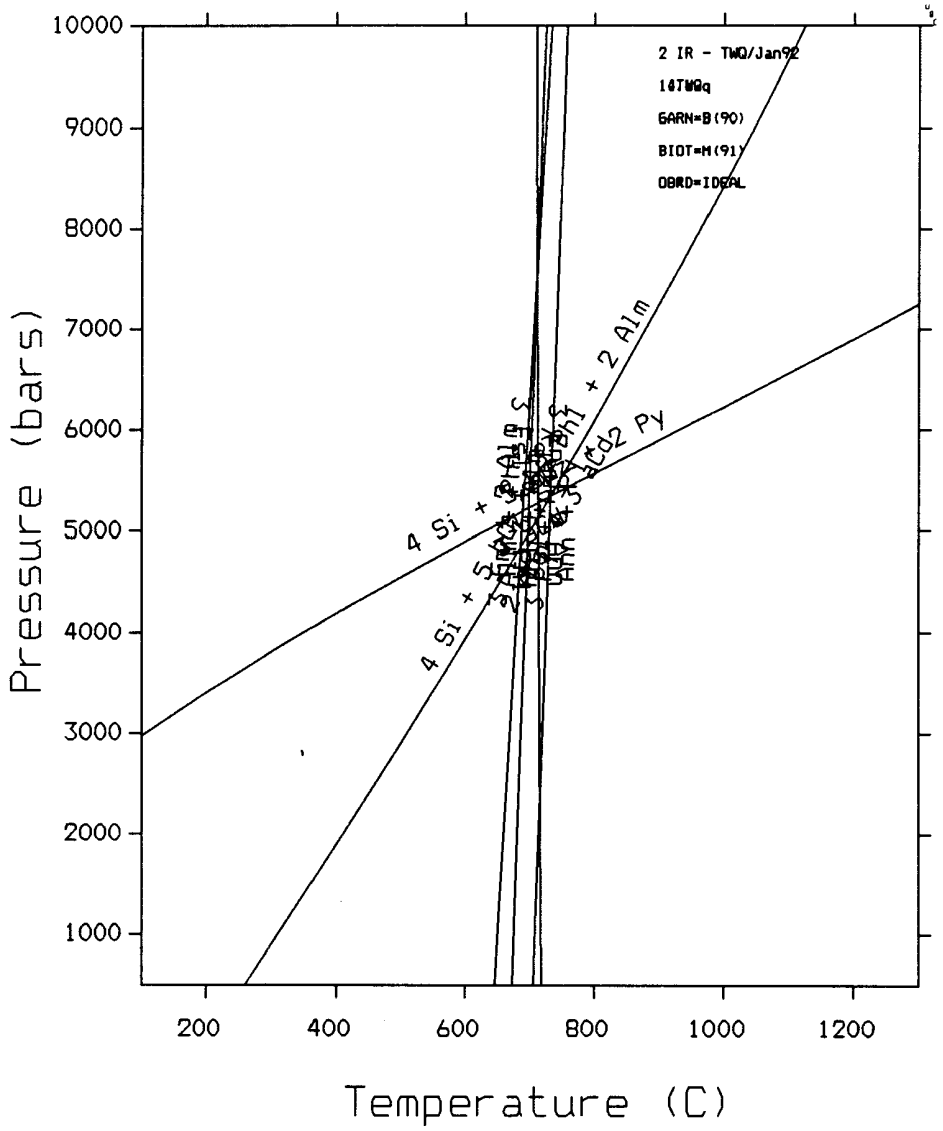

Figure 7a: TWEEQU plot from sample 3, representing core compositions

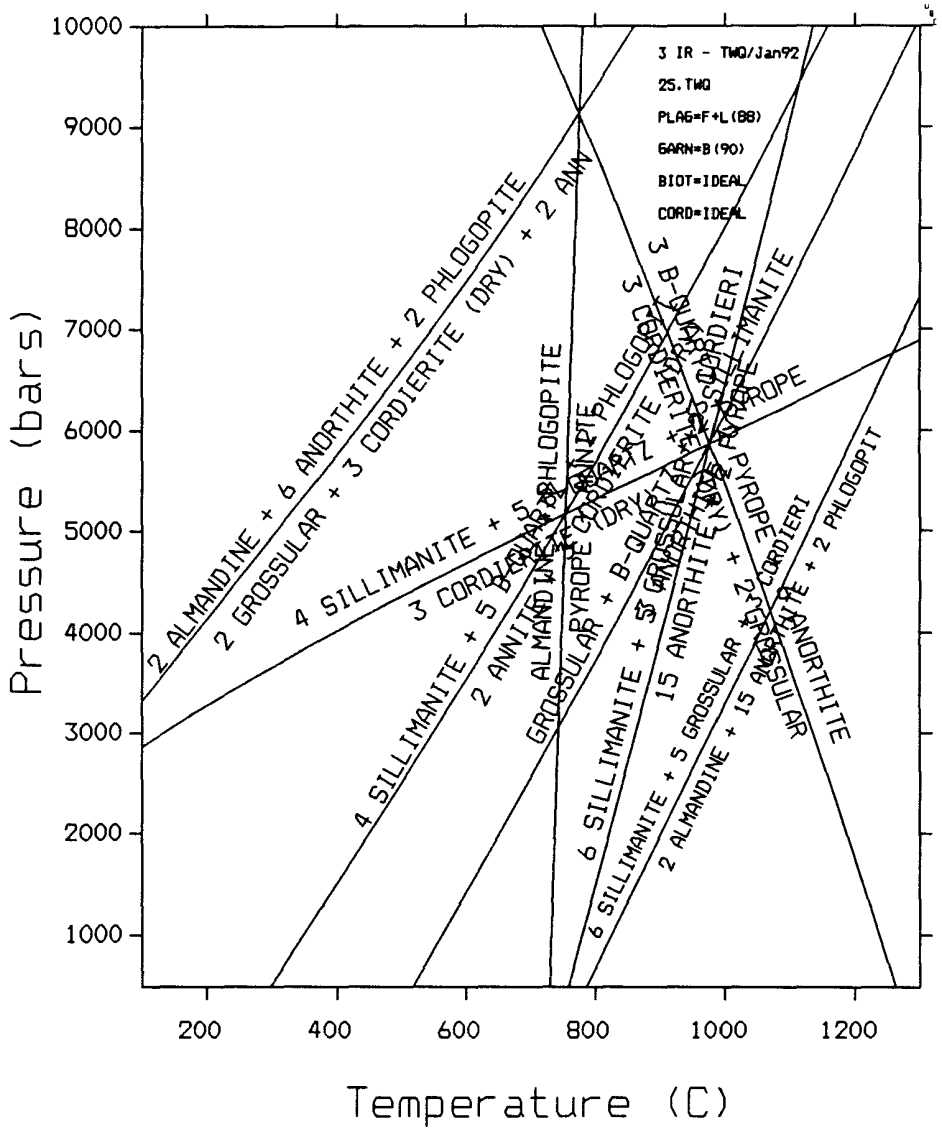

Figure 7b: TWEEQU plot from sample 3, representing rim compositions

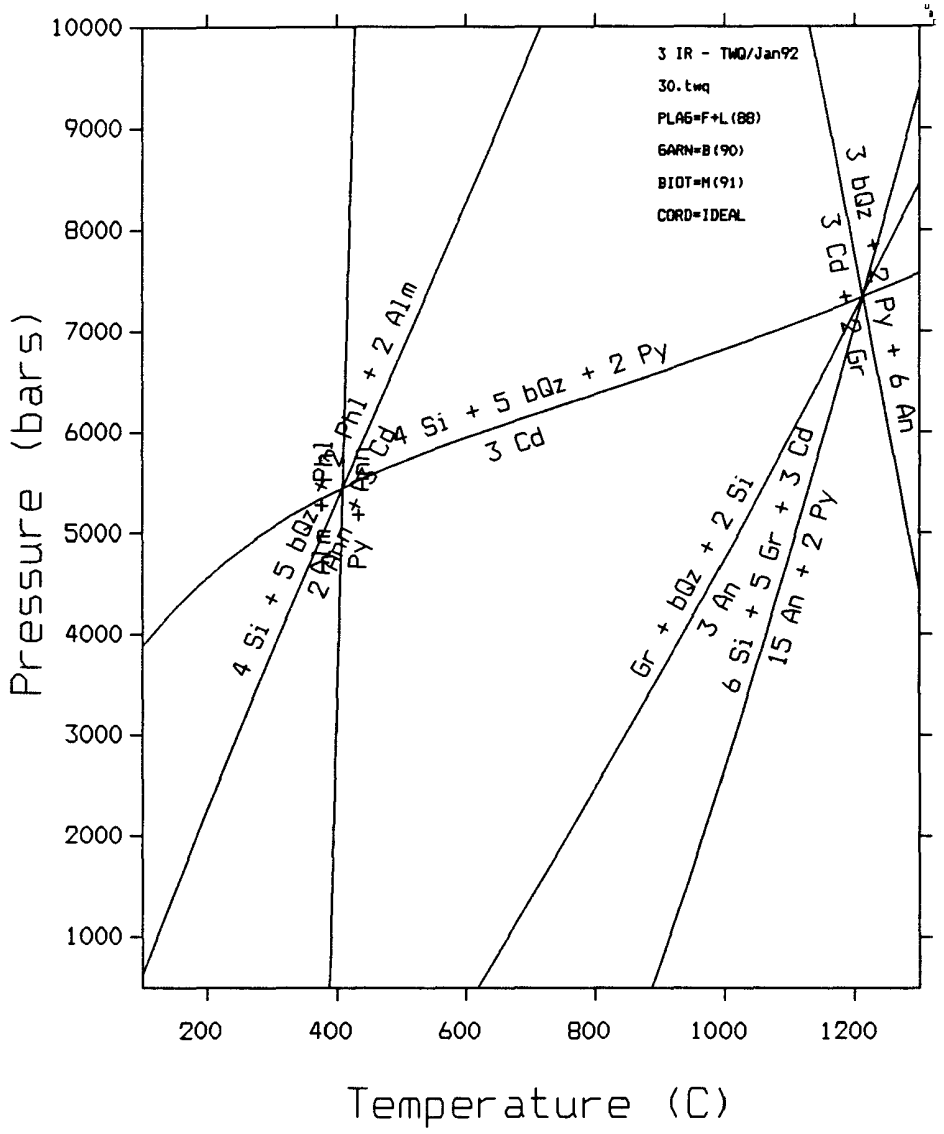

Figure 7c: TWEEQU plot from sample 3, representing core compositions, and **increased** anorthite

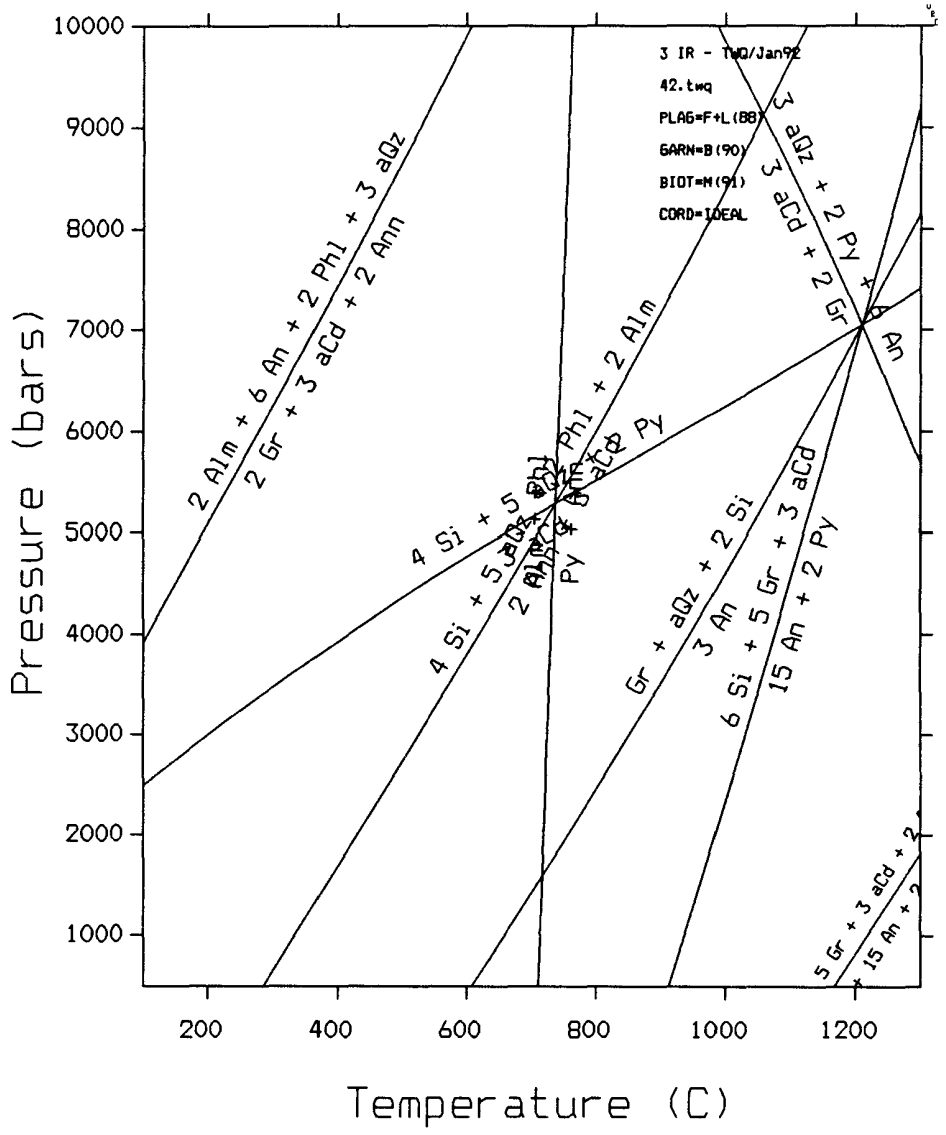

Figure 7d: TWEEQU plot from sample 3, representing core compositions, and **decreased** anorthite

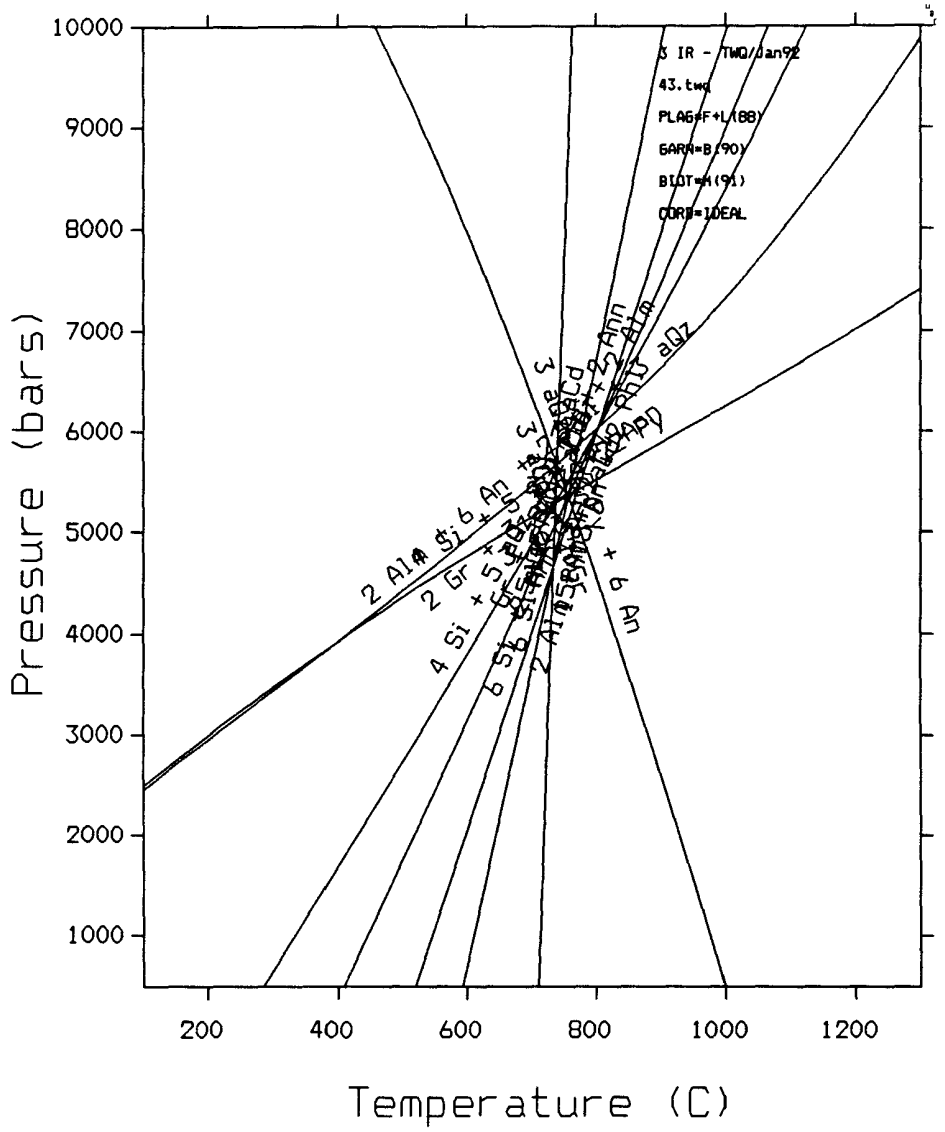

Figure 8: TWEEQU plot from sample 3, representing core compositions with garnet recalculated to account for ferric iron

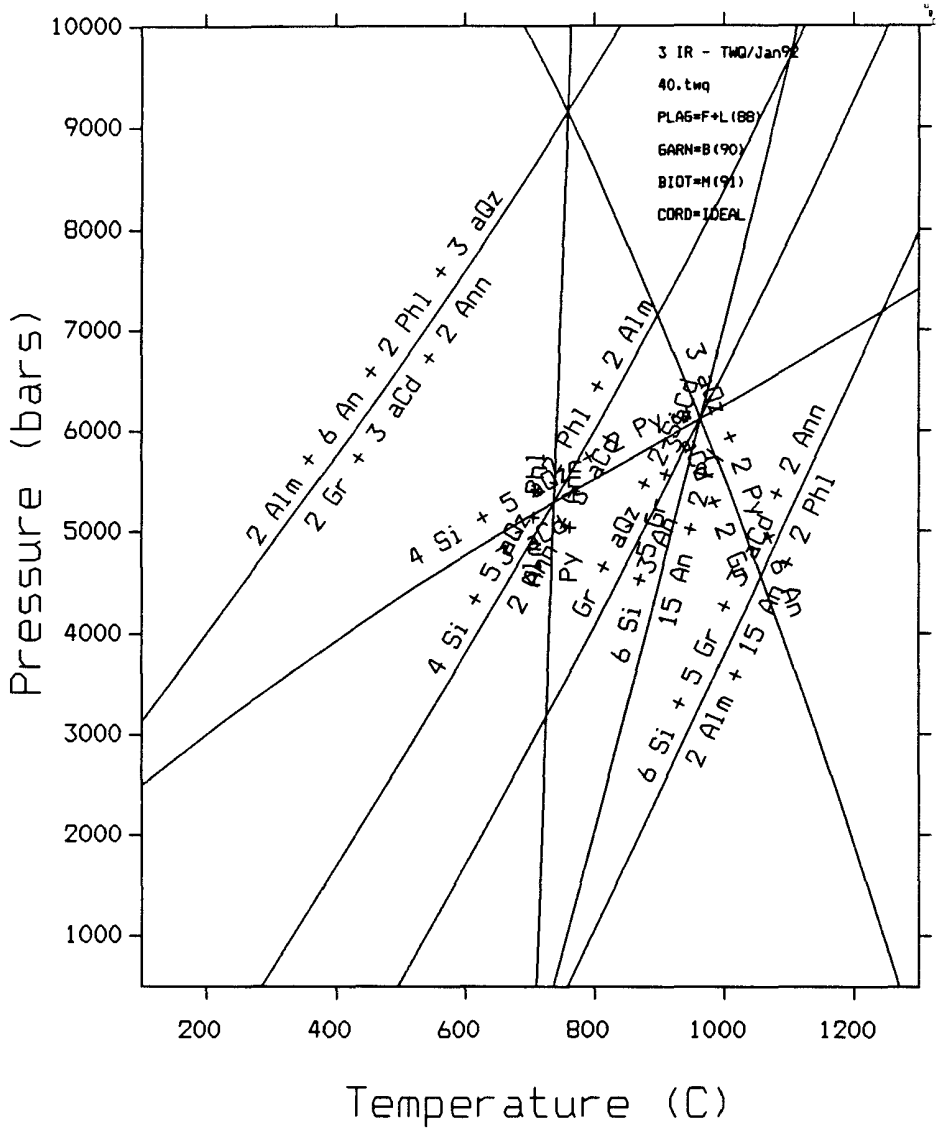

The P-T-t Path

Maximum thermobarometric estimates obtained in this study are in within the limits of previous qualitative estimates made based on phase equilibria. Jansen et al. (1980) estimated temperatures for the M2 stage near the osumilite-in isograd (figure 1) from where these samples were collected, to be around 800°C at the peak of metamorphism. Additionally, peak temperatures from this study roughly concur with the quantitative estimates obtained by Miller et al. (1992, see figure 3). Peak pressures from this study are higher than those earlier obtained, and are midway between the two pressure range estimates made based on phase equilibria (see figure 2). Rim analyses agree with the isobaric cooling model for M3 (figure 3). The results from the samples analyzed in this study are consistent with a regional interpretation involving crustal thickening, and associated heating, rather than higher temperatures that might be expected if the granulite facies represented a contact metamorphic zone associated with the anorthite intrusion.

CONCLUSION

Understanding the nature of granulite petrogenesis is dependent on well-constrained estimates of the temperature and pressure conditions during metamorphism. Results obtained in this study are thought to represent the granulite facies peak or near peak metamorphic conditions for M2 in SW Norway because: 1) the results are consistent with the general known conditions for granulite metamorphism; 2) the results are also consistent with

qualitative estimates made for the region based on phase equilibria; 3) they essentially agree with previous quantitative temperature and pressure estimates obtained from nearby granulites.

More quantitative work needs to be done in this region to better characterize the pressure and temperature of the amphibolite-granulite facies transition. This study shows that through careful, detailed analysis, estimates of peak M2 metamorphic conditions can be calculated, in spite of widespread M3 equilibration, and contrary to some previous work (eg. Jansen et al., 1985; Kars et al., 1980). Results from this study are consistent with a clockwise P-T-t path, and the corresponding model for granulite facies metamorphism in SW Norway based on continent-continent collision.

Acknowlegements

I am greatly indebted to Kip Miller for his patient instruction throughout this project. I also want to thank Mike Barton for advising me, and Michael Comerford for his assistance.

Appendix A

Sample analyses

BIOTITE

	SiO2	Al2O3	TiO2	FeO	MnO	MgO	CaO	Na2O	K2O	TOTAL
gr1 core1	38.042	14.238	4.558	13.045	0.000	16.054	0.000	0.000	10.331	97.735
gr1 core2	37.671	14.230	4.569	12.747	0.000	16.065	0.000	0.000	10.306	95.588
gr1 core3	38.525	13.976	4.638	12.900	0.000	15.895	0.000	0.000	10.255	96.189
gr1 core av	38.079	14.148	4.588	12.897	0.000	16.005	0.000	0.000	10.297	96.504
gr1 rim1	38.126	14.074	4.487	12.447	0.000	16.094	0.000	0.000	10.250	95.478
gr1 rim2	38.331	13.989	4.360	12.141	0.000	16.137	0.000	0.000	10.380	95.338
gr1 rim3	38.873	14.000	4.218	11.915	0.000	16.649	0.000	0.000	10.497	96.152
gr1 rim av	38.443	14.021	4.355	12.168	0.000	16.293	0.000	0.000	10.376	95.656
gr2 core1	37.885	14.037	4.251	14.135	0.000	15.926	0.000	0.000	9.890	96.124
gr2 core2	37.219	14.010	4.215	13.487	0.000	15.833	0.000	0.000	9.866	94.630
gr2 core3	37.366	14.058	4.561	13.181	0.000	16.164	0.000	0.000	10.182	95.512
gr2 core av	37.490	14.035	4.342	13.601	0.000	15.974	0.000	0.000	9.979	95.422
gr2 rim1	37.605	14.093	4.493	12.703	0.000	16.235	0.000	0.000	10.503	95.632
gr2 rim2	37.017	14.036	3.773	14.171	0.000	15.737	0.000	0.000	9.190	93.924
gr2 rim3	37.561	13.882	4.365	12.494	0.000	16.331	0.000	0.000	10.161	94.794
gr2 rim av	37.394	14.004	4.210	13.123	0.000	16.101	0.000	0.000	9.951	94.783

ORTHOPYROXENE

	SiO2	TiO2	Al2O3	Cr2O3	MgO	CaO	MnO	FeO	NiO	Na2O	Total
gr1 core1	45.813	0.194	6.219	0.024	15.171	0.146	0.344	31.047	0.000	0.018	98.976
gr1 core2	46.197	0.268	6.047	0.062	15.276	0.161	0.423	31.585	0.000	0.039	100.057
gr1 core3	46.419	0.218	6.053	0.052	15.089	0.140	0.349	32.139	0.000	0.036	100.495
gr1 core av	46.143	0.227	6.106	0.046	15.179	0.149	0.372	31.590	0.000	0.031	99.843
gr1 rim1	48.982	0.152	5.810	0.037	14.997	0.261	0.327	29.659	0.000	0.025	100.250
gr1 rim2	46.622	0.160	5.991	0.026	15.206	0.138	0.368	31.120	0.000	0.014	99.644
gr1 rim3	46.135	0.111	5.801	0.000	15.148	0.333	0.309	29.788	0.000	0.022	97.648
gr1 rim av	47.246	0.141	5.867	0.021	15.117	0.244	0.335	30.189	0.000	0.020	99.181
gr2 core1	46.566	0.201	6.249	0.041	16.531	0.149	0.307	28.981	0.000	0.003	99.029
gr2 core3	46.704	0.208	6.119	0.000	16.791	0.118	0.254	28.707	0.000	0.030	98.932
gr2 core av	46.635	0.205	6.184	0.021	16.661	0.134	0.281	28.844	0.000	0.017	98.981
gr2 rim1	47.271	0.161	5.396	0.032	17.259	0.156	0.245	28.962	0.000	0.044	99.527
gr2 rim2	47.530	0.144	5.281	0.028	16.995	0.172	0.276	28.786	0.000	0.011	99.223
gr2 rim3	47.072	0.191	5.004	0.028	16.814	0.142	0.303	28.998	0.000	0.016	98.567
gr2 rim av	47.291	0.165	5.227	0.029	17.023	0.157	0.275	28.915	0.000	0.024	99.106
gr3 core1	46.375	0.173	5.739	0.054	15.363	0.135	0.362	30.479	0.000	0.014	98.694
gr3 core2	46.601	0.123	5.663	0.030	15.545	0.128	0.354	30.519	0.000	0.018	98.981
gr3 core3	46.230	0.150	5.776	0.034	15.327	0.156	0.402	30.827	0.000	0.000	98.902
gr3 core av	46.402	0.149	5.726	0.039	15.412	0.140	0.373	30.608	0.000	0.011	98.859
gr3 rim1	44.595	0.128	5.448	0.013	15.658	0.137	0.366	30.935	0.000	0.009	97.290
gr3 rim2	45.585	0.171	5.976	0.073	16.216	0.152	0.352	30.126	0.000	0.024	98.675
gr3 rim3	46.342	0.251	5.069	0.060	16.339	0.135	0.391	29.918	0.000	0.025	98.529
gr3 rim av	45.507	0.183	5.498	0.049	16.071	0.141	0.370	30.326	0.000	0.019	98.165

PLAGIOCLASE

	SiO2	Al2O3	MgO	CaO	FeO	BaO	Na2O	K2O	Total
gr1 sp1	58.232	26.026	0.870	6.690	1.071	0.000	6.895	0.310	100.096
gr1 sp2	58.973	26.283	0.000	7.802	0.071	0.194	6.975	0.117	100.414
gr1 sp3	59.242	26.059	0.000	7.909	0.067	0.000	7.100	0.145	100.522
gr1 sp4	59.295	26.124	0.000	7.736	0.095	0.000	7.108	0.142	100.500
gr1 av	59.170	26.155	0.000	7.816	0.078	0.065	7.061	0.135	100.479
gr2 sp1	59.381	25.934	0.000	7.864	0.098	0.038	7.078	0.131	100.524
gr2 sp2	59.184	25.747	0.000	7.869	0.142	0.000	7.226	0.148	100.316
gr2 sp3	60.059	25.945	0.000	7.065	0.064	0.000	7.527	0.080	100.740
gr2 av	59.541	25.875	0.000	7.599	0.101	0.013	7.277	0.120	100.527
gr3 sp1	59.144	25.868	0.000	7.707	0.138	0.000	7.157	0.119	100.133
gr3 sp2	59.526	25.724	0.000	7.734	0.101	0.000	7.189	0.128	100.403
gr3 sp3	59.257	25.846	0.000	7.665	0.199	0.206	7.044	0.109	100.325
gr3 sp4	59.195	26.044	0.000	7.864	0.142	0.034	7.115	0.117	100.512
gr 3 av	59.288	25.879	0.000	7.768	0.127	0.011	7.154	0.121	100.349
gr4 sp1	59.320	26.045	0.000	7.911	0.098	0.027	7.062	0.113	100.576
gr4 sp2	58.891	25.965	0.000	8.003	0.159	0.000	6.886	0.149	100.053

gr4	sp3	57.663	25.825	0.503	6.797	1.151	0.217	6.625	0.563	99.343
gr4	sp4	59.372	26.415	0.000	7.912	0.138	0.050	7.095	0.174	101.156
gr4	av	59.346	26.230	0.000	7.912	0.118	0.038	7.078	0.144	100.866
gr5	sp1	59.141	25.352	0.000	7.629	0.037	0.000	7.088	0.192	99.439
gr5	sp2	58.780	25.833	0.000	7.514	0.007	0.053	7.122	0.184	99.492
gr5	sp3	59.660	25.542	0.000	7.552	0.047	0.000	7.273	0.138	100.213
gr5	sp4	59.331	25.490	0.000	7.770	0.014	0.095	7.088	0.152	99.940
gr5	sp5	58.749	25.155	0.000	7.806	0.115	0.015	7.155	0.139	99.134
gr5	av	59.063	25.510	0.000	7.624	0.056	0.023	7.183	0.154	99.613
gr6	sp1	58.388	26.030		8.146	0.162		6.795	0.176	99.696
gr6	sp2	58.667	26.175		8.018	0.071	0.084	6.941	0.172	100.128
gr6	av	58.528	26.102	0.000	8.082	0.116	0.042	6.868	0.174	99.910

CORDIERITE

		SiO2	TiO2	Al2O3	MgO	CaO	MnO	FeO	Na2O	K2O	Total
gr1	core1	48.502	0.015	32.440	10.433	0.007	0.000	6.043	0.512	0.017	97.969
gr1	core2	49.226	0.003	32.969	9.214	0.032	0.066	7.456	0.268	0.000	99.233
gr1	core av	48.864	0.009	32.705	9.824	0.020	0.033	6.750	0.390	0.009	98.601
gr1	rim	48.952	0.006	32.747	8.732	0.153	0.000	6.689	0.872	0.000	98.152
gr1	av	48.908	0.008	32.726	9.278	0.086	0.017	6.719	0.631	0.004	98.377
gr2	core1	49.418	0.000	32.615	9.604	0.000	0.066	7.164	0.287	0.007	99.162
gr2	core2	48.929	0.005	33.257	9.568	0.000	0.032	6.883	0.245	0.006	98.925
gr2	core3	49.265	0.000	33.388	9.686	0.014	0.024	7.150	0.059	0.001	99.585
gr2	core av	49.204	0.002	33.087	9.619	0.005	0.041	7.066	0.197	0.005	99.224
gr2	rim1	49.175	0.012	33.080	9.241	0.024	0.058	7.246	0.414	0.017	99.267
gr2	rim2	48.990	0.000	32.480	9.487	0.028	0.013	7.131	0.057	0.012	98.197
gr2	rim3	48.972	0.003	33.056	9.297	0.013	0.040	6.951	0.248	0.010	98.590
gr2	rim av	49.046	0.005	32.872	9.342	0.022	0.037	7.109	0.240	0.013	98.685
gr2	av	49.125	0.003	32.979	9.481	0.013	0.039	7.088	0.218	0.009	98.954
gr3	core1	48.923	0.009	32.999	10.196	0.012	0.032	6.080	0.172	0.000	98.423
gr3	core2	48.318	0.000	33.309	9.643	0.000	0.000	6.824	0.309	0.003	98.408
gr3	core3	48.422	0.004	32.108	9.562	0.005	0.063	7.054	0.081	0.002	97.301
gr3	core av	48.554	0.004	32.805	9.800	0.006	0.032	6.653	0.187	0.002	98.044
gr3	rim1	49.004	0.005	32.938	10.444	0.000	0.011	6.394	0.108	0.010	98.914
gr3	rim2	49.215	0.000	32.598	10.287	0.009	0.000	6.372	0.030	0.002	98.512
gr3	rim3	48.605	0.012	33.359	10.130	0.016	0.032	6.650	0.116	0.015	98.934
gr3	rim av	48.941	0.006	32.965	10.287	0.008	0.014	6.472	0.085	0.009	98.787
gr3	av	48.748	0.005	32.885	10.044	0.007	0.023	6.562	0.136	0.005	98.415

SILLIMANITE

		SiO2	Al2O3	MgO	CaO	FeO	Na2O	K2O	Total
gr1	core1	36.703	63.481	0.014	0.007	0.343	0.011	0.020	100.577
gr1	core2	36.868	63.485	0.007	0.003	0.328	0.000	0.007	100.700
gr1	core3	37.420	63.621	0.005	0.001	0.364	0.007	0.000	101.417
gr1	av	36.997	63.529	0.009	0.004	0.345	0.006	0.009	100.898
gr2	sp1	36.703	63.481	0.014	0.007	0.343	0.011	0.020	100.577
gr2	sp2	36.868	63.485	0.007	0.003	0.328	0.000	0.007	100.700
gr2	sp3	37.420	63.621	0.005	0.001	0.364	0.007	0.000	101.417
gr2	av	36.997	63.529	0.009	0.004	0.345	0.006	0.009	100.898
gr3	sp1	37.949	64.082	0.005	0.100	0.296	0.000	0.007	102.349
gr3	sp2	36.269	63.329	0.014	0.018	0.393	0.011	0.006	100.041
gr3	sp3	36.705	62.661	0.015	0.000	0.313	0.012	0.006	99.712

GARNET

		FEO	SIO2	CAO	MNO	AL2O3	TIO2	MGO	CR2O3	Total
gr1	core1	31.546	37.805	1.212	0.781	22.654	0.061	7.105	0.016	101.180
gr1	core2	31.236	37.607	1.213	0.923	22.612	0.021	7.202	0.068	100.880
gr1	core3	31.381	38.155	1.179	0.824	22.824	0.043	7.264	0.018	101.689
gr1	core	31.388	37.856	1.201	0.843	22.697	0.042	7.190	0.034	101.250
gr1	core av	31.560	37.823	1.208	0.863	22.771	0.029	7.298	0.023	101.576
gr1	rim1	31.204	37.977	1.346	0.910	22.934	0.013	7.149	0.082	101.615
gr1	rim2	31.341	38.012	1.320	0.883	22.869	0.006	7.146	0.018	101.595
gr1	rim3	31.512	37.394	1.277	0.824	22.837	0.031	7.146	0.050	101.071
gr1	rim av	31.352	37.794	1.314	0.872	22.880	0.017	7.147	0.050	101.427
gr2	core1	31.255	37.157	1.192	0.791	22.657	0.021	7.428	0.016	100.516
gr2	core2	31.516	37.426	1.193	0.786	22.828	0.006	7.313	0.014	101.081
gr2	core3	31.605	37.362	1.172	0.767	22.778	0.043	7.267	0.000	100.994

gr2 core av	31.459	37.315	1.186	0.781	22.754	0.023	7.336	0.010	100.864
gr2 rim1	31.148	37.436	1.296	0.786	22.725	0.002	7.288	0.052	100.733
gr2 rim2	31.409	37.620	1.284	0.764	22.795	0.039	7.283	0.064	101.257
gr2 rim3	31.019	37.499	1.329	0.788	22.891	0.033	7.249	0.022	100.830
gr2 rim av	31.192	37.518	1.303	0.779	22.804	0.025	7.273	0.046	100.940
gr3 core1	31.869	37.354	1.168	0.739	22.799	0.026	7.068	0.022	101.046
gr3 core 2	31.456	37.542	1.154	0.855	22.896	0.053	7.058	0.044	101.057
gr3 core av	31.663	37.448	1.161	0.797	22.848	0.040	7.063	0.033	101.052
gr3 rim 1	30.970	37.334	1.285	0.829	22.642	0.036	7.027	0.042	100.165
gr3 rim 2	31.079	36.908	1.286	0.869	22.750	0.004	7.091	0.000	99.987
gr3 rim av	31.025	37.121	1.286	0.849	22.696	0.020	7.059	0.021	100.076
section core	31.517	37.611	1.189	0.821	22.767	0.033	7.222	0.025	101.185
section rim	31.258	37.500	1.291	0.838	22.798	0.022	7.171	0.042	100.920
section av	31.388	37.555	1.240	0.829	22.783	0.028	7.196	0.033	101.053

Appendix B

Thin section descriptions

Sample 1: Section of a course-grained, banded cordierite-garnet gneiss. Primary minerals include garnet (6-12 mm diameter; 25%), cordierite (1-3 mm, 20%), quartz (1-3 mm, 20%), sillimanite (0.5-1 mm, 10%), and biotite (0.5-2 mm, 10%). Secondary alteration (mainly serecite) comprises about 10-15% of section. Accessory minerals include rutile, sphene, zircon, and minor pyrite.

Tectonnically elongated anhedral garnet porphyroblasts contain inclusions of quartz, biotite, oxide phases, and microlaths of what is possibly plagioclase. These microlaths display a preferred orientation, with long axes parallel to the elongation of the garnet grains themselves.

Euhedral cordierite display twinning and contain pleochroic haloes around inclusions of zircon and sphene. Cordierite usually is in close association with quartz, and is the apparent parent for most of the secondary alteration occurring in the section.

Sillimanite occurs in both the fibrous and anhedral crystal form. The fibrous form appears to be a secondary product.

Biotite grains are euhedral in shape and are marginally altered.

Sample 2: Section is of a medium to course grained granoblastic plagioclase-garnet gneiss. Primary minerals include plagioclase (1-3 mm, 25%), garnet (2-4 mm, 20%), quartz (1-3 mm, 25%), orthopyroxene (1-3 mm, 10%), and biotite (0.5 mm-2 mm, 10%). Secondary alteration (serecite) makes up about 10% of section. Accessory mineral include rutile, zircon, and sphene.

Euhedral garnet porphyroblasts contain inclusions of quartz, biotite, and plagioclase. They frequently are intergrown with orthopyroxene, and are marginally altered.

Plagioclase crystals frequently contain quartz and are highly altered.

Orthopyroxene crystals are anhedral and are usually in contact with altered garnets.

Biotite grains are generally lath shaped and do not appear to be highly altered.

Sample 3: Section is of a course-grained cordierite-garnet gneiss. Primary minerals include garnet (4-10 mm, 25%), cordierite (1-2 mm, 20%), quartz (1-2 mm, 15%), biotite (0.5-2 mm, 10%), sillimanite (0.5-2 mm, 10%), and plagioclase (0.5-1 mm, 5%). Secondary alteration (serecite) makes up about 5% of section. Accessory minerals include illmanite, rutile, sphene, and hercynite.

Tectonically elongated garnet porphyroblasts contain inclusions of quartz and biotite, and minor oxide phases.

Cordierite contains pleochroic haloes around inclusions of zircon and sphene, and comprises most of the alteration occurring in section.

Myrmekite occurs where plagioclase is in contact with quartz. Plagioclase appears as discreet laths, marginally altered.

Symplektite intergrowth also occurs between sphene and hercynite

REFERENCES

Barton M, Van Bergen MJ (1984) Secondary ilvaite in a dolerite dike from Rogaland, SW Norway. Mineral Mag 48: 449-456

Barton M, Van Gaans C (1988) Formation of orthopyroxene-Fe-Ti oxide symplectites in Precambrian intrusives, southwestern Norway. Am Mineral 73: 1046-1059

Barton M, Comerford MC, Drent HP (1991) Retrograde metamorphism of noritic-monozonoritic dikes, Rogaland/Vest Agder, SW Norway: Petrology, geochemistry,and element mobility. J Petro, in press

Berman RG (1991) Thermobarometry using multi-equilibrium calculations: A new technique, with petrological applications. Canadian Mineralogist 29: 833-855

Bohlen SR (1991) On the formation of granulites. J Metamorphic Geol 9: 223-229

Brown TH, Berman RG, Perkins EH (1988) GEO-CALC: software package for calculation and display of pressure-temperature-composition phase diagrams using an IBM or compatible personal computer. Comput & Geosci 14: 279-289

Demaiffe D, Michot J (1985) Isotope geochronology of the Proterozoic crustal segment of southern Norway: A review. In: Tobi AC, Touret JLR (eds) The deep Proterozoic crust in the North Atlantic Provinces. Reidel, Dordrecht, pp 441-434

Gaal G, Gorbatschev R (1989) An outline of the Precambrian evolution of the Baltic Shield. Precambrian Research 35: 15-52

Griffin WL, O'Reilly SY (1986) Ultramafic xenoliths from the Mt. Carmel area (Karem Maharal Volcano), Isr Lithos 19: 42-49

Hermans GAEM, Tobi AC, Poorter RPE, Maijer C (1975) The high-grade metamorphic Precambrian of Rogaland, SW Norway. Norges Geol Unders 318: 51-74

Huijsmans JPP, Barton M, Van Bergen MJ (1982) A pegmatite containing Fe-rich grandodierite, Ti-rich dumortietite and tourmaline from the Precambrian high-grade metamorphic complex of Rogaland, SW Norway. N Jb Mineral Abh 143: 149-261

Jansen JBH, Blok RJP, Bos A, Scheelings M (1985) Geothermometry and geobarometry in Rogaland and preliminary results from the Bamble area, South Norway. In: Tobi AC, Touret JLR (eds) The Deep Proteroxoic crust in the North Atlantic Provinces. Reidel, Dordrecht, pp 499-516

Kars H, Jansen JBH, Tobi AC, Poorter RPE (1980) The metapelitic rocks of the polymetamorphic Precambrian of Rogaland, SW Norway - Part 2. Mineral relations between cordierite, hercynite and magnetite within the osumilite-in isograd. Contrib Mineral Pterol 74: 235-244

Maijer C, Andriessen PAM, Hebeda EH, Jansen JBH, Verschure RH (1981) Osumilite, an approximately 970 Ma old high-temperature index mineral of the granulite-facies metamorphism in Rogaland, SW Norway. Geol Mijnb 60: 267-272

McGuire AV, Dyar MD, Ward KA (1989) Neglected Fe^{3+}/Fe^{2+} ratios - a study of Fe^{3+} content of megacrysts from alkali basalts. Geology 17: 687-690

Miller CA, Comerford M, Barton M (1992) P-T-a_{H2O} estimates for granulite-facies metamorphism and subsequent amphibolite-facies retrograde metamorphism in Rogaland, SW Norway. Geol Soc Amer Abstracts with Programs. Annual Meeting, 1992

Newton RC (1990) Fluids and melting in the Archaian deep crust of southern India. In: Ashworth JR, Brown M (eds) High-temperature metamorphism and crustal anatexis. Unwin Hyman, London, pp 149-179

Rietmeijer FMJ (1984) Pyroxene (re-)equilibration in the Precambrian terrain of SW Norway between 1030-990 Ma and reinterpretation of events during regional cooling (M3stage). Norsk Geol Tidssk 64: 7-20

Sauter Pcc, Hermans GAEM, Jansen JBH, Maijer C, Spits P, Weglin A (1983) Polyphase Caledonian metamorphism in the Precambrian basement of Rogaland/Vest Agder, Southwest Norway. Norges Geol Unders 380: 7-22

Thompson AB (1990) Heat, fluids, and melting in the granulite facies. In: Vielzeuf D, Vidal, Ph (eds) Granulites and crustal evolution. Kluwer, Dordrecht, pp 37-57

Tobi AC, Hermans GAEM, Maijer C, Jansen JBH (1985) Metamorphic zoning in the high-grade Proterozoic of Rogaland/Vest-Agder. In: Tobi AC, Touret JLR (eds) The deep Proterozoic crust in the North Atlantic Provinces. Reidel, Dordrecht, pp 477-497

Vlaar NJ (1985) Precambrian geodynamical constraints. In: Tobi AC, Touret JLR (eds) The deep Proterozoic crust in the North Atlantic Provinces. Reidel, Dordrecht, pp 3-20

Wilmart E, Duchesne JC (1987) Geothermobarometry of igneous and metamorphic rocks around the Åna-Sira anorthosite massif: Implications for the depth of emplacement of the South Norwegian anorthosite. Norsk Geol Tidsskr 67: 185-196